HHS Public Access

Author manuscript

ChemMedChem. Author manuscript; available in PMC 2016 February 01.

Published in final edited form as:

ChemMedChem. 2015 February ; 10(2): 253–265. doi:10.1002/cmdc.201402453.

Optimization of 1,2,5-Thiadiazole Carbamates as Potent and Selective ABHD6 Inhibitors [#]

Mr. Jayendra Z. Patel[*,a], **Dr. Tapio J. Nevalainen**[a], **Dr. Juha R. Savinainen**[b], **Mr. Yahaya Adams**[a], **Dr. Tuomo Laitinen**[a], **Mr. Robert S. Runyon**[c], **Ms. Miia Vaara**[b], **Mr. Stephen Ahenkorah**[a], **Dr. Agnieszka A. Kaczor**[a,d], **Ms. Dina Navia-Paldanius**[b], **Dr. Mikko Gynther**[a], **Ms. Niina Aaltonen**[a], **Dr. Amit A. Joharapurkar**[e], **Dr. Mukul R. Jain**[e], **Dr. Abigail S. Haka**[c], **Prof. Frederick R. Maxfield**[c], **Dr. Jarmo T. Laitinen**[b], and **Dr. Teija Parkkari**[*,a]

[a]School of Pharmacy, University of Eastern Finland, P.O.Box 1627, FI-70211 Kuopio (Finland), Fax: (+358) 17-162-456 [b]School of Medicine, Institute of Biomedicine/Physiology, University of Eastern Finland, P.O. Box 1627, FIN-70211 Kuopio, Finland [c]Department of Biochemistry, Weill Cornell Medical College, 1300 York Avenue, New York, NY 10065, USA [d]Department of Synthesis and Chemical Technology of Pharmaceutical Substances, Faculty of Pharmacy with Division of Medical Analytics, Medical University of Lublin, 4a Chodzki St., PL-20093 Lublin, Poland [e]Department of Pharmacology & Toxicology, Zydus Research Centre, Sarkhej Bavla NH8A, Moraiya, Ahmedabad-382210, Gujarat, India

Abstract

At present, inhibitors of α/β-hydrolase domain 6 (ABHD6) are viewed as a promising approach to treat inflammation and metabolic disorders. This article describes the optimization of 1,2,5-thiadiazole carbamates as ABHD6 inhibitors. Altogether, 34 compounds were synthesized and their inhibitory activity was tested using lysates of HEK293 cells transiently expressing human ABHD6 (hABHD6). Among the compound series, 4-morpholino-1,2,5-thiadiazol-3-yl cyclooctyl(methyl)carbamate (JZP-430, **55**) potently and irreversibly inhibited hABHD6 (IC_{50} 44 nM) and showed good selectivity (∼230 fold) over fatty acid amide hydrolase (FAAH) and lysosomal acid lipase (LAL), the main off-targets of related compounds. Additionally, activity-

[#]J.Z.P dedicates this article to mentor Saurin Raval (Ph.D.), a principal scientist in Medicinal Chemistry Department at Zydus Research Centre, Ahmedabad-382210, Gujarat, India

[*]Corresponding author: Phone: +358-40-3553887, Fax: +358-17-162424, jayendra.patel@uef.fi, jayorgchem137@gmail.com (JZP), teija.parkkari@uef.fi (TP).

Supporting information for this article is available on the WWW under http://www.chemmedchem.org

Supporting Information: The supporting information covers the following data: Synthesis and spectroscopic characterization of all intermediates (**8-21**); elemental analyses for all final compounds (**22-55**); determination of MAGL activity using 2-AG as a substrate; determination of ABHD12 activity using a previously validated sensitive fluorescent glycerol assay; determination of lipophilicity values for the compounds **52-55**; determination of LAL inhibitory activity (IC_{50}); TAMRA-FP labelling in mouse brain proteome through competitive ABPP assay; cannabinoid receptor activity; molecular modelling studies and related references. This material is available free of charge via the Internet at http://www.chemmedchem.org.

Author Contributions: The manuscript was written through contributions of all authors. All authors have given approval to the final version of the manuscript.

Notes: The authors declare no competing financial interest.

based protein profiling (ABPP) indicated that compound **55** (JZP-430) displayed good selectivity among the serine hydrolases of mouse brain membrane proteome.

Keywords

2-arachidonoylglycerol; enzymes; inhibitors; human α/β hydrolase domain 6; 1,2,5-thiadiazole carbamate; human recombinant fatty acid amide hydrolase; human recombinant monoacylglycerol lipase; human α/β hydrolase domain 12; activity-based protein profiling

Introduction

In the central nervous system (CNS), the α/β hydrolase domain containing 6 (ABHD6), an integral membrane serine hydrolase, contributes to a small portion of the *in vivo* degradation of 2-arachidonoylglycerol (2-AG), an endogenous lipid signaling molecule activating the cannabinoid receptors.[1] At the bulk brain level, ABHD6 along with the serine hydrolases monoacylglycerol lipase (MAGL) and α/β hydrolase domain containing 12 (ABHD12) account for ∼98% of 2-AG degradation; [2] 85% of 2-AG is metabolized by MAGL and 9% by ABHD12 while only 4% is attributed to ABHD6.[2] The remaining ∼2% is hydrolyzed by additional enzymes, including fatty acid amide hydrolase (FAAH). MAGL, ABHD12 and ABHD6 have different tissue distribution and subcellular localization, suggesting that they may have distinct roles in controlling the lifetime of 2-AG.[1] In order to distinguish between these roles and to gain in-depth understanding of their physiological significance, selective ABHD6 inhibitors are needed.

Recent reports have suggested ABHD6 as an emerging therapeutic target for the treatment of inflammation, metabolic disorders (obesity and type II diabetes mellitus) and epilepsy.[3-6] ABHD6 inhibitors may have certain advantages over inhibitors of MAGL and ABHD12. First, genetic inactivation of MAGL causes a massive increase in brain 2-AG levels, leading to psychotropic side effects and cannabinoid receptor desensitization.[7-9] Second, even though ABHD12 is still poorly characterized, studies with genetically ABHD12 deficient mice suggest that inactivation of this serine hydrolase leads to age-dependent symptoms that resemble the human neurodegenerative disorder PHARC (polyneuropathy, hearing loss, ataxia, retinosis pigmentosa, cataract).[10] Inhibition of ABHD6, on the other hand, is expected to induce only a slight increase in 2-AG levels suggesting that ABHD6 inhibitors may have less CNS-related side-effects.[2,4,11]

To date, only a few ABHD6 inhibitors have been reported (Figure 1). In 2007, the Cravatt laboratory reported the identification of WWL70 (**1**), a potent and selective carbamate-based inhibitor whose selectivity among the serine hydrolases was evaluated using activity-based protein profiling (ABPP).[12] Marrs and colleagues described UCM710 (**2**), a dual inhibitor of ABHD6 and FAAH.[13] Examples of non-selective ABHD6 inhibitors include methylarachidonoyl fluorophosphonate (MAFP), orlistat (tetrahydrolipstatin, THL, **3**), RHC-80267, and the triterpene pristimerin.[14] Recently, the Cravatt laboratory disclosed several other ABHD6 inhibitors such as carbamate based compound WWL123 (**4**), an isoster analogue of WWL70, and triazole urea analogues (e.g. KT195 (**5**) and KT182 (**6**)) as potent and selective ABHD6 inhibitors.[15-17] Very recently, Janssen et. al. reported

glycine sulfonamide analogue LEI-106 (**7**) as dual inhibitor of sn-1-diacylglycerol lipase α (DAGL-α)and ABHD6.[18]

In 2010, Helquist and coworkers reported 1,2,5-thiadiazole carbamates (I, Figure 2) as potent inhibitors of lysosomal acid lipase (LAL, also known as LIPA).[19] LAL has been recently identified as a potential therapeutic target for Niemann-Pick disease type C (NPC), a condition characterized by a gradual lysosomal accumulation of lipids such as cholesteryl esters and triglycerides. Additionally, Helquist and colleagues reported that orlistat (**3**), which acts as a broad-spectrum lipase inhibitor, also inhibits LAL. So far, numerous carbamate compounds have been reported as inhibitors of endocannabinoid metabolizing enzymes,[12,15,20-23] (for recent reviews, see [24-27]). We therefore thought to utilize 1,2,5-thiadiazole carbamate (I, Figure 2) scaffold for the development of inhibitors of the endocannabinoid metabolizing enzymes. A limited structure-activity relationship (SAR) study based on this scaffold has been reported [19], thus leaving room for further optimization of the 1,2,5-thiadiazole carbamate scaffold (II, Figure 2). The mechanism for LAL inhibition via 1,2,5-thiadiazole carbamates is suggested to occur by carbamylation of the active site serine with the 1,2,5-thiadiazole alcohol group serving as the leaving group (I, Figure 2). In our compound series (Figures 2 and 3), we utilized 1,2,5-thiadiazole scaffold by introducing different cyclic and non-cyclic secondary amines at the main core while a small set of different cyclic amines were introduced as potential leaving groups.

In this paper, we report the optimization of 1,2,5-thiadiazole carbamates as novel ABHD6 inhibitors. The selectivity against other endocannabinoid targets, serine hydrolases of the mouse membrane proteome as well as LAL has been evaluated, and the inhibitory activity data have been used to explore the SAR. Finally, homology modeling and molecular docking were used in attempts to provide insight into how the best compounds interacted optimally with the active site of ABHD6.

Results and Discussion

The synthesis of 1,2,5-thiadiazole carbamates (**22-55**) is shown in Scheme 1. Commercially available 3,4-dichloro-1,2,5-thiadiazole was coupled with the appropriate secondary amine to afford a corresponding monochloro 1,2,5-thiadiazole derivative (**8-14**), which was then converted to 1,2,5-thiadiazole alcohol (**15-21**) via treatment with aqueous alkali. Finally, coupling with appropriate carbamoyl chloride gave the desired 1,2,5-thiadiazole carbamates (**22-55**). The synthesis of monochloro 1,2,5-thiadiazole derivatives (**8-14**), 1,2,5-thiadiazole alcohol derivatives (**15-21**) and carbamoyl chloride compounds was performed as per literature procedures with minor modifications (see Supporting Information).

SAR of ABHD6 Inhibitors

The inhibitory activities of the synthesized compounds were initially screened at 1 μM concentration against hABHD6 and hABHD12, and at 10 μM concentration against hFAAH and hMAGL. As FAAH was found to be the main off-target, inhibitory activity data concerning hABHD6 and hFAAH are presented in Tables 1-4, while results of the hABHD12 and hMAGL inhibition experiments are presented in Tables S3 and S4 (see Supplementary Information).

(A) Cyclic '*N*' Containing Thiadiazole Carbamates (Structural Modifications of Main Core and Leaving Group)—As an initial step, we synthesized two previously reported LAL inhibitors having piperidine and morpholine rings at opposite sides of the thiadiazole core, i.e. compounds **22** and **23** (Table 1). Both **22** and **23** showed excellent ABHD6 inhibitory activities with potencies in the low nanomolar range (IC_{50} 52 nM and 85 nM, respectively) but these compounds inhibited also FAAH with moderate potencies (IC_{50} 0.40 and 0.30 μM, respectively). As compound **22** was more potent of these two we retained the thiadiazole piperidine core in the newly synthesized analogues **24** and **25**. We found a similar inhibitory activity trend for pyrrolidine analogue **24** and 1,2,3,4-tetrahydroisoquinoline analogue **25**, although decreased inhibitory potencies towards ABHD6 and FAAH were observed. Since none of the analogues showed significant improvement in selectivity, we clarified the effect of the leaving group by synthesizing different thiadiazole carbamates (**26-30**) in which the piperidine carbamate scaffold was kept intact. Substituted piperidine analogues **26** and **28** as well as piperazine analogue of **26** (compound **27**) showed similar FAAH inhibition, while only weak inhibition of ABHD6 was observed. However, fused bicyclic analogues (compounds **29** and **30**) showed improved FAAH inhibition (IC_{50} 17 nM and 31 nM, respectively) while moderate inhibitory activities were observed against ABHD6 (IC_{50} 0.46 and 0.56 μM, respectively). Compounds **22-30** did not show any appreciable inhibition of hMAGL or hABHD12 (Table S3, Supporting Information).

In order to reveal additional off-targets, we screened selected analogues (**22, 23, 29** and **30**) at 1 μM concentration against the serine hydrolases of the mouse brain membrane proteome using competitive ABPP, essentially as previously described [14,28] (Figure S1, see Supporting Information). We found that all the tested compounds showed complete inhibition of FAAH, and inhibition of ABHD6 was also evident. Moreover, an unidentified serine hydrolase (a protein band migrating at ∼30 kDa) was found as an off-target of the four analogues.

(B) Non-Cyclic '*N*' Containing Thiadiazole Carbamates (Structural Modifications of the Main Core)—As no satisfactory selectivity for ABHD6 over FAAH was achieved with the analogues **22-30** (selectivity-ratio < 30-fold), we explored the thiadiazole carbamates further by opening the '*N*' containing ring system in the main core (see Figure 2). *N*,*N*-dimethyl analogue **31** showed weak FAAH inhibition (IC_{50} 6.45 μM) while no inhibition was seen against the other tested enzymes (Table 2 and Tables S3-S4). Replacing one methyl group of **31** with a phenyl group (compound **32**) resulted in excellent ABHD6 inhibitory activity (IC_{50} 22 nM), and also improved ABHD6 selectivity (404-fold) over FAAH (IC_{50} 8.9 μM). However, adding another phenyl group in the compound **32** (compound **33**) resulted in complete loss of activity towards all the tested enzymes. Additionally, the *N*,*N*-diisopropyl analogue (compound **34**) showed loss of activity, which may be due to shielding of the carbonyl group from attack by the serine hydroxyl group at the active site of the enzyme. As compound **32** turned out to be the best ABHD6 inhibitor, we investigated further the optimal structural requirement needed for inhibitory activity and selectivity. Changing the methyl group of the compound **32** into an ethyl (compound **35**) resulted in a ∼20-fold drop in potency, while changing the phenyl (**32**) into benzyl (**36**)

resulted in a 2-fold increase in ABHD6 inhibitory activity (IC_{50} 10 nM). Compound **35** showed no noticeable inhibition of the other tested enzymes (Table 2 and Table S3 in Supporting Information), while loss of selectivity was observed for compound **36** as it also showed improved FAAH inhibition (IC_{50} 67 nM) as well as weak MAGL inhibition (IC_{50} 5.6 μM, see Table S3 in Supporting Information).

In competitive ABPP of the mouse brain membrane proteome, compounds **32** and **36** were found to inhibit ABHD6 completely (Figure S2, Supporting Information) at 1 μM concentration. As expected, **36** also targeted FAAH. In addition, an unidentified serine hydrolase (a protein band migrating at ∼30 kDa) was inhibited by **32**.

(I) *N*-Methyl-*N*-Substituted Phenyl Thiadiazole Carbamates: Next, we investigated the effect of different substituents on the phenyl ring of compound 32 by synthesizing the analogues **37-51** (Table 3). Among these, compounds having an electron withdrawing group (EWG) at the *para* position of the phenyl ring (compounds **37, 41** and **42**) showed a 4- to 55-fold loss of ABHD6 inhibitory activity, and the cyano analogue **40** showed complete loss of activity. Switching the *para*-nitro substituent (compound **37**) to the *meta* position (compound **38**) retained activity, while in the *ortho* position (compound **39**) ABHD6 inhibitory activity was completely lost. Furthermore, both *para*- and *meta*-fluoro analogues (compounds **42** and **43**) were almost equipotent in inhibiting ABHD6. In a similar fashion, electron donating groups (EDG) at the *para*-position resulted in a 6- to 12-fold loss of ABHD6 inhibitory activity, depending on the nature of EDG (**44** and **47**). However, switching back the methyl substituent from the *para* (**44**) to the *meta* position (**45**) showed almost a 3-fold improvement in ABHD6 inhibition, while methoxy analogues (compounds **47** and **48**) showed only marginal differences in their ABHD6 inhibitory activities. However, their *ortho* analogues (**46** and **49**) showed complete loss of ABHD6 inhibition. Finally, substitution of the phenyl ring with the *meta*-phenyl resulted in almost a 40-fold loss (compound **50**) of ABHD6 inhibitory potency, and the bulky trimethyl substitution (compound **51**) lead to complete loss of activity. None of the analogues **37-51** showed appreciable inhibition of hFAAH, hMAGL or hABHD12 (Table 3 and Table S4 in Supporting Information).

To screen inhibitor selectivity among the serine hydrolases in mouse brain membrane proteome, we performed competitive ABPP for selected analogues (**42** and **45**) and found complete inhibition of ABHD6 at 1 μM concentration (Figure S3, Supporting Information). In addition, an unidentified serine hydrolase migrating at ∼30 kDa was targeted by the compounds **42** and **45**.

(II) *N*-Methyl-*N*-Cycloalkyl Thiadiazole Carbamates: Since no further improvement in ABHD6 inhibitory activity or selectivity was obtained with the analogues **37-51**, we replaced the phenyl ring of compound **32** by different cycloalkyl rings (compounds **52-55**, Table 4). Increasing the size of the cycloalkyl ring from a six- to eight-membered ring (**52-54**) resulted in approximately a 2-4-fold loss of ABHD6 inhibition, while interestingly no inhibition of FAAH was observed at 10 μM. As increased ring size also causes increased lipophilicity (i.e. cLogP for **52** is 4.4 while for **54** it is 5.5, see supporting information, Table

S5), we replaced the piperidine ring of compound **54** with a morpholine ring (compound 55). Consequently, compound **55** had comparable ABHD6 inhibitory activity to compounds **52** and **53** along with being less lipophilic (cLogP = 4.1). None of these compounds **52-55** showed any inhibition of the other enzymes tested (Table S4, Supporting Information). Finally, when these analogues (**52-55**) were tested using competitive ABPP, all the compounds except compound **52** selectively targeted ABHD6 when tested at 1 μM concentration (Figure S4, Supporting Information). Compound **52** additionally targeted the ∼30 kDa serine hydrolase with unknown identity.

ABHD6 Selectivity

(I) LAL Inhibitory Activity—As our compound series was developed from the compounds that were originally designed as LAL inhibitors, we tested the activity of these compounds towards LAL, essentially as previously described.[19] We selected several potent analogues (**22, 23, 29, 30, 32, 36, 42, 45** and **52-55**) from our compound series containing both known LAL inhibitors as well as novel ABHD6 inhibitors, and tested them at 10 μM concentration. (Figure 4). Among the cyclic analogues (**22, 23, 29** and **30**) the previously reported LAL inhibitors **22** and **23** were found to inhibit LAL activity almost completely. A similar trend was observed for our compounds **29** and **30**, both having bulky cyclic rings as potential leaving groups. Among the non-cyclic analogues (**32, 36, 42, 45** and **52-55**), *N*-methyl-*N*-aryl analogues **32, 42** and **45** were found to inhibit LAL activity by 25-35%, and interestingly, *N*-methyl-*N*-benzyl analogue **36** showed > 99% inhibition. *N*-methyl-*N*-cycloalkyl analogues **52-55** were also weak LAL inhibitors showing < 33% inhibition at 10 μM concentration. Notably, the ABHD6 inhibitor **55** (JZP-430) was found to have only a slight inhibition (< 20%) of LAL at 10 μM concentration. We determined the dose-responses and calculated the IC_{50} values for those compounds that in the initial screen showed >50% inhibition (Table S6, Supplementary Information).

(II) Activity Based Protein Profiling (ABPP)—Next, we tested in more detail the selectivity of our carbamate-based analogue JZP-430 (**55**) using competitive ABPP of the mouse brain membrane proteome (Figure 5). We used earlier reported inhibitors WWL70 (**1**) [12] and JZP-327A [29] at the indicated concentrations to locate the bands of ABHD6 and FAAH, respectively. We found that JZP-430 (**55**) inhibited ABHD6 dose-dependently, being effective already at 0.25 μM concentration. Selective inhibition of ABHD6 was detected even at 1 μM concentration while negligible inhibition of FAAH was observed at 2.5 μM concentration. At 20-fold (5 μM) concentration partial inhibition of FAAH was detected. In short, when tested at below 2.5 μM concentration, JZP-430 (**55**) appeared to be selective for ABHD6 over the other detectable brain serine hydrolases, including FAAH, MAGL and ABHD12.

(III) Selectivity Over the Other Endocannabinoid Targets—Finally, JZP-430 (**55**) was tested against the cannabinoid CB_1 and CB_2 receptors but it did not show any appreciable agonist or antagonist activity when tested at 10 μM concentration (Table S7, Supporting Information).

Reversibility of ABHD6 Inhibition

To get deeper insight into ABHD6-binding mode of JZP-430 (**55**), we tested its potency to inhibit ABHD6 using a 96-well format dilution method.[28] As a result, both the established irreversible ABHD6 inhibitor WWL70 (**1**) and JZP-430 (**55**) fully retained their potencies during the 90 min incubation period following a fast 40-fold dilution of the enzyme-inhibitor complex (Figure 6), a finding suggesting that compound **55** inactivated hABHD6 in an irreversible manner

Molecular Modeling

We assumed in our homology- modeling studies that the catalytic triad of ABHD6 comprises Ser^{148}-His^{306}-Asp^{278} and the oxyanion hole is formed by Met^{149} and Phe^{80}.[14] A homology model of ABHD6 has been successfully used in docking studies.[31] Our comparative modeling studies suggested that among the current template structures available, template pdb: 2XMZ [32] resulted in optimal active site geometry for docking studies.

The docking poses of highest affinity support the idea that bulkiness at the main core and leaving group modulate the selectivity for ABHD6 over FAAH. In the case of ABHD6, compounds **54** and **55** (JZP-430), which have larger cyclic rings at the main core, provide a shape complementary with the active site cavity of our model (Figure 7). In addition, the piperidine/morpholine rings dock well to the other end of the L-shaped site. However, the *N*-containing bicyclic rings of compounds **29** and **30** seem to be too rigid and thus failed to dock at this position. As a consequence, modeling studies suggest that good inhibitory activity is gained when proper shape complementarity meets easy access for the carbonyl to oxyanion hole prior to nucleophilic attack. Compounds **54** and **55** (JZP-430) have more spacious aliphatic ring structures located in this narrower region of the FAAH active site, so no converged docking poses were found. When examining the interaction of compounds **29** and **30** with FAAH, the bulkiest *N*-containing bicyclic ring system was found to dock to the entrances of the acyl binding site and membrane access channel, while the piperidine/morpholine rings fit well in the mouth of the cytoplasm exit (Figure S5, Supporting Information).

Conclusions

In this study, we have identified 1,2,5-thiadiazole carbamates as novel ABHD6 inhibitors and used molecular modeling to define their interactions with the catalytic site of the enzyme. The best compound of the series, in terms of both potency and selectivity, was 4-morpholino-1,2,5-thiadiazol-3-yl cyclooctyl(methyl)carbamate (JZP-430, **55**), as this compound inhibited human α/β hydrolase domain 6 (hABHD6) with low-nanomolar potency (IC_{50} 44 nM) and was > 200-fold selective for ABHD6 over FAAH and LAL enzymes. Moreover, compound **55** showed good selectivity for ABHD6 over the other serine hydrolases detected in the mouse brain membrane proteome using ABPP. Compound **55** (JZP-430) showed irreversible binding in our reversibility assays and in molecular modeling studies, it was docked well into the active site of hABHD6 and was shown to have

favorable interactions, including important hydrogen-bonding of the carbonyl oxygen, to the oxyanion hole.

Experimental Section

Material and methods

Reagents and solvents were purchased from commercial suppliers and were used without further purification. Reactions were monitored by thin-layer chromatography using aluminium sheets coated with silica gel F_{245} (60 Å, 40-63 μm, 230-400 mesh) with suitable UV visualization. Purification was carried out by flash chromatography (FC) on J. T. Baker's silica gel for chromatography (pore size 60 Å, particle size 50 nm). Petroleum ether (PE) used for chromatography is of fraction 40–60 °C. ^{1}H NMR and ^{13}C NMR were recorded on a Bruker Avance AV 500 (Bruker Biospin, Switzerland) spectrometer operating on 500.1 and 125.8 MHz, respectively. Tetramethylsilane (TMS) was used as an internal standard for ^{1}H NMR. Chemical shifts are reported in ppm on the δ scale from an internal standard of solvent ($CDCl_3$ 7.26 and 77.0 ppm, DMSO 2.50). The spectra were processed from the recorded FID files with TOPSPIN 2.1 software. Following abbreviations are used: s, singlet; br s, broad singlet; d, doublet; t, triplet; q, quartet; m, multiplet. Coupling constants are reported in Hz. ESI-MS spectra were acquired using a LCQ quadrupole ion trap mass spectrometer equipped with an electrospray ionization source (Thermo LTQ, San Jose, CA, USA). Elemental analyses were performed on a ThermoQuest CE instrument (EA 1110 CHNS-O) or a Perkin-Elmer PE 2400 Series II CHNS-O Analyzer.

General procedures for preparation of 1,2,5-thiadiazole carbamates (22-55) [19]

To a solution of 1,2,5-thiadiazole alcohol (1.0 equiv) in dry THF (0.2 M) was added KOtBu (1.3 equiv) at 0 °C. The mixture was stirred at the same temperature for 10-30 min. Carbamoyl chloride (1.0 equiv) was added slowly under inert atmosphere. The reaction mixture was allowed to warm and stirred at 20-25 °C for another 16-24 h. The progress of the reaction was monitored by TLC using 20% EtOAc in PE as a mobile phase. Reaction mixture was diluted with EtOAc. It was washed with H_2O and brine. The organic layer was dried over sodium sulphate, filtered and concentrated under vacuum to afford crude 1,2,5-thiadiazole carbamates which were purified by flash column chromatography using PE: EtOAc (9: 1) as an eluent. The desired fractions were collected and solvents were evaporated on a rotatory evaporator to afford 1,2,5-thiadiazole carbamates. The obtained solid 1,2,5-thiadiazole carbamate was stirred in minimum amount of solvent (n-hexane or di-isopropyl ether (DIPE)) for 10-12 minutes and, filtered and dried. The purity of the synthesized 1,2,5-thiadiazole carbamates (**22-55**) were determined through combustion analyses and are ≥ 95% (see Table S1 and S2 of Supplementary Information).

4-(Piperidin-1-yl)-1,2,5-thiadiazol-3-yl morpholine-4-carboxylate (22)

White solid (270 mg, 56%); ^{1}H NMR ($CDCl_3$): δ 3.74-3.70 (br s, 4H), 3.66-3.62 (br s, 2H), 3.55-3.51 (br s, 2H), 3.37-3.35 (m, 4H), 1.64-1.60 (m, 6H); ^{13}C NMR ($CDCl_3$): δ 153.7, 150.9, 146.2, 66.6, 66.4, 49 (2C), 45.2, 44.5, 25.4 (2C), 24.2; ESI-MS: 299.05 $[M + H]^+$

4-Morpholino-1,2,5-thiadiazol-3-yl piperidine-1-carboxylate (23)

White solid (190 mg, 42%); ^{1}H NMR ($CDCl_3$): δ 3.81-3.79 (m, 4H), 3.59-3.57 (m, 2H), 3.54-3.53 (m, 2H), 3.45-3.44 (m, 4H), 1.69-1.57 (m, 6H); ^{13}C NMR ($CDCl_3$): δ 153.1, 150.8, 146.7, 66.3 (2C), 48.1 (2C), 46, 45.6, 26, 25.4, 24; ESI-MS: 299.02 $[M + H]^+$

4-(Piperidin-1-yl)-1,2,5-thiadiazol-3-yl pyrrolidine-1-carboxylate (24)

White solid product (55 mg, 12%); ^{1}H NMR ($CDCl_3$): δ 3.58-3.55 (m, 2H), 3.53-3.50 (m, 2H), 3.43-3.40 (m, 4H), 2.0-1.93 (m, 4H), 1.67-1.62 (m, 6H); ^{13}C NMR ($CDCl_3$): δ 153.7, 150.3, 146.6, 49 (2C), 46.8, 46.7, 29.7, 25.8, 25.4, 24.9, 24.2; ESI-MS: 283.22 $[M + H]^+$

4-(Piperidin-1-yl)-1,2,5-thiadiazol-3-yl 3,4-dihydroisoquinoline-2(1H)-carboxylate (25)

Brown oil (90 mg, 62%); ^{1}H NMR ($CDCl_3$): δ 7.24-7.10 (m, 4H), 4.79 (s, 1H), 4.71 (s, 1H), 3.87 (t, J = 5.6 Hz, 1H), 3.81 (t, J = 5.6 Hz, 1H), 3.38-3.35 (m, 4H), 2.95 (t, J = 5.9 Hz, 2H), 1.65-1.59 (m, 6H); ^{13}C NMR ($CDCl_3$): δ 153.7, 151.2, 146.4, 134.6, 132.5, 128.9, 127, 126.7, 126.4, 49, 46.5, 42.6, 38.7, 30, 25.9, 25.4, 24.4; ESI-MS: 345.64 $[M + H]^+$

4-(4-Phenylpiperidin-1-yl)-1,2,5-thiadiazol-3-yl piperidine-1-carboxylate (26)

White solid product (542 mg, 42%); ^{1}H NMR ($CDCl_3$): δ 7.30 (t, J = 7.5 Hz, 2H), 7.21 (t, J = 8.3, 3H), 4.13-4.07 (m, 2H), 3.57-3.55 (br s, 2H), 3.54-3.50 (br s, 2H), 3.03-2.97 (m, 2H), 2.72-2.68 (m, 1H), 1.92-1.80 (m, 4H), 1.65-1.61 (m, 4H), 1.56-1.52 (m, 2H); ^{13}C NMR ($CDCl_3$): δ 153.5, 150.8, 146.7, 145.6, 128.5 (2C), 126.7 (2C), 126.4, 48.7 (2C), 45.9, 45.5, 42.4, 32.9, 32.8, 26, 25.4, 24; ESI-MS: 373.25 $[M + H]^+$

4-(4-Phenylpiperazin-1-yl)-1,2,5-thiadiazol-3-yl piperidine-1- carboxylate (27)

White solid (63 mg, 8%); ^{1}H NMR ($CDCl_3$): δ 7.26 (t, J = 8.0 Hz, 2H), 6.94 (d, J = 7.9 Hz, 2H), 6.88 (t, J = 7.3 Hz, 1H), 3.60-3.58 (m, 6H), 3.53-3.49 (br s, 2H), 3.27-3.25 (m, 4H), 1.67-1.63 (br s, 6H); ^{13}C NMR ($CDCl_3$): δ 153.1, 151.1, 150.8, 147.2, 129.2 (2C), 120.4, 116.5 (2C), 49 (2C), 47.9 (2C), 46, 45.6, 26, 25.4, 24.1; ESI-MS: 374.21 $[M + H]^+$

4-(4-Benzylpiperidin-1-yl)-1,2,5-thiadiazol-3-yl piperidine-1-carboxylate (28)

White solid (134 mg, 31%); ^{1}H NMR (DMSO): δ 7.27 (t, J = 7.5 Hz, 2H), 7.17 (t, J = 7.0 Hz, 3H), 4.02 (s, 1H), 3.86 (d, J = 12.8 Hz, 2H), 3.56-3.51 (br s, 2H), 3.43-3.38 (br s, 2H), 3.32-3.28 (m, 1H), 2.83 (t, J = 11.9 Hz, 2H), 2.53-2.51 (m, 2H), 1.75-1.71 (m, 1H), 1.63-1.52 (m, 6H), 1.27-1.19 (m, 2H); ^{13}C NMR ($CDCl_3$): δ 153.5, 150.8, 146.6, 140.2, 129.1 (2C), 128.3 (2C), 126, 48.3, 46, 45.5, 43.1, 37.8, 31.6 (2C), 29.7, 26, 25.4, 24.1; ESI-MS: 387.23 $[M + H]^+$

4-(3,4-Dihydroisoquinoline-2-(1H)-yl)-1,2,5-thiadiazole-3-yl piperidine-1-Carboxylate (29)

Off white solid (230 mg, 42%); ^{1}H NMR ($CDCl_3$): δ 7.18-7.09 (m, 4H), 4.67 (s, 2H), 3.75 (t, J = 5.7 Hz, 2H), 3.65-3.61 (br s, 2H) 3.55-3.51 (br s, 2H), 2.96 (t, J = 5.9 Hz, 2H), 1.68-1.64 (m, 6H); ^{13}C NMR ($CDCl_3$): δ 152.8, 150.9, 146.2, 134, 133.4, 128.8, 126.5, 126.3 (2C), 49.7, 46, 45.6, 45.3, 28.7, 26, 25.4, 24.1; ESI-MS: 345.19 $[M + H]^+$

4-(Octahydroisoquinoline-2-(1H)-yl)-1,2,5-thiadiazole-3-yl piperidine-1- carboxylate (30)

White solid (200 mg, 68%); ^{1}H NMR (DMSO): δ 3.93-3.90 (br s, 1H), 3.75-3-72 (br s, 1H), 3.54 (d, *J* = 4.8 Hz, 2H), 3.40 (d, *J* = 5.3 Hz, 2H), 2.87 (t, *J* = 12.4 Hz, 1H), 2.54-2.51 (m, 1H), 1.69-1.65 (m, 2H), 1.59-1.48 (m, 9H), 1.25-1.06 (m, 5H), 0.97-0.90 (m, 2H); ^{13}C NMR (CDCl3): δ 153.5, 150.8, 146.5, 54.3, 48.8, 45.9, 45.5, 41.8, 41.5, 32.9, 32.4, 30.1, 26.3, 26, 25.9, 25.4, 24.1; ESI-MS: 351.23 [M + H]$^{+}$

4-(Piperidin-1-yl)-1,2,5-thiadiazol-3-yl dimethylcarbamate (31)

White solid (220 mg, 79%); ^{1}H NMR ($CDCl_3$): δ 3.41-3.39 (m, 4H), 3.11 (s, 3H), 3.04 (s, 3H), 1.66-1.62 (m, 6H); ^{13}C NMR ($CDCl_3$): δ 153.6, 152.1, 146.5, 48.9 (2C), 37, 36.6, 25.3, 25.1, 24.1; ESI-MS: 257.04 [M + H]$^{+}$

4-(Piperidin-1-yl)-1,2,5-thiadiazol-3-yl methyl(phenyl)carbamate (32)

White solid (132 mg, 38%); ^{1}H NMR ($CDCl_3$): δ 7.42-7.39 (m, 2H), 7.32-7.25 (m, 3H), 3.43-3.38 (br s, 4H), 3.17 (s, 3H), 1.57-1.55 (br s, 6H); ^{13}C NMR ($CDCl_3$): δ 153.4, 151, 146.2, 142, 129.3 (2C), 127.6 (2C), 126.4, 48.8 (2C), 38.7, 25.4, 25.1, 24.2; ESI-MS: 319.04 [M + H]$^{+}$

4-(Piperidin-1-yl)-1,2,5-thiadiazol-3-yl diphenylcarbamate (33)

White solid (273 mg, 88%); ^{1}H NMR ($CDCl_3$): δ 7.38-7.36 (m, 8H), 7.27-7.25 (m, 2H), 3.24-3.20 (br s, 4H), 1.61-1.56 (br s, 6H); ^{13}C NMR ($CDCl_3$): δ 153.6, 150.1, 145.9, 141.4 (2C), 129.2 (8C), 127 (2C), 48.9, 48.7, 25.5, 25.3, 24.1; ESI-MS: 381.03 [M + H]$^{+}$

4-(Piperidin-1-yl)-1,2,5-thiadiazol-3-yl diisopropylcarbamate (34)

Brown oil (627 mg, 36%); ^{1}H NMR ($CDCl_3$): δ 4.63-4.12 (br s, 1H), 3.93-3.91 (br s, 1H), 3.40 (t, *J* = 5.3 Hz 4H), 1.68-1.59 (m, 6H), 1.33-1.29 (m, 12H); ^{13}C NMR ($CDCl_3$): δ 153.9, 150.4, 146.5, 48.7 (2C), 47.2, 46.8, 25.1 (4C), 24, 21.1, 20.1; ESI-MS: 313.63 [M + H]$^{+}$

4-(Piperidin-1-yl)-1,2,5-thiadiazole-3-yl ethyl(phenyl)carbamate (35)

White solid (160 mg, 18 %); ^{1}H NMR ($CDCl_3$): δ 7.43-7.27 (m, 5H), 3.83-3.78 (br s, 2H), 3.18-3.15 (br s, 4H), 1.56-1.52 (br s, 6H), 1.25-1.16 (m, 3H); ^{13}C NMR ($CDCl_3$): δ 153.4, 150.5, 146.2, 140.3, 129.3, 129.1, 127.8, 127.6, 48.8, 46.2, 25.5, 25.4 (2C), 24.8,24.1, 13; ESI-MS: 333.06 [M+H]$^{+}$

4-(Piperidin-1-yl)-1,2,5-thiadiazol-3-yl benzyl(methyl)carbamate (36)

White solid (450 mg, 35%). ^{1}H NMR ($CDCl_3$): δ 7.38-7.26 (m, 5H), 4.61 (d, *J*= 2.7 Hz, 1H), 4.56 (d, *J*= 2.9 Hz, 1H) 3.40-3.32 (m, 4H), 3.30 (s, 3H), 1.58-1.54 (m, 6H); ^{13}C NMR ($CDCl_3$): δ 153.8, 152.2, 146.5, 136.2, 128.8, 127.9, 127.8, 127.1, 53.2, 49, 35.2, 34.2, 29.7, 25.3 (2C), 24.2; ESI-MS: 333.08 [M+H]$^{+}$

4-(Piperidin-1-yl)-1,2,5-thiadiazol-3-yl methyl(4-nitrophenyl)carbamate (37)

White solid (410 g, 70%); ^{1}H NMR ($CDCl_3$): δ 8.28 (d, *J* = 8.95 Hz, 2H), 7.56 (d, *J* = 8.81 Hz, 2H), 3.52 (s, 3H), 3.31-3.26 (br s, 4H), 1.62-1.57 (br s, 6H); ^{13}C NMR ($CDCl_3$): δ

153.5, 150.5, 147.6, 145.6, 144.5, 126.4, 125.9 (2C), 124.6 (2C), 49 (2C), 38.1, 25.5, 25.3, 24; ESI-MS: 364.03 $[M + H]^+$

4-(Piperidin-1-yl)-1,2,5-thiadiazol-3-yl methyl(3-nitrophenyl)carbamate (38)

Yellow solid (406 mg, 52%); ^{1}H NMR ($CDCl_3$): δ 8.25-8.19 (m, 2H), 7.77-7.62 (m, 2H), 3.54-3.50 (br s, 4H), 3.28 (s, 3H), 1.62-1.57 (br s, 6H); ^{13}C NMR ($CDCl_3$): δ 153.5, 150.7, 148.7, 145.7, 143.1, 132.3, 130.1, 122.2, 121.3, 49.3, 49, 38.4, 25.5, 25.3, 24.1; ESI-MS: 364.04 $[M + H]^+$

4-(Piperidin-1-yl)-1,2,5-thiadiazol-3-yl methyl(2-nitrophenyl)carbamate (39)

Brown oil (1.3 g, 66%); ^{1}H NMR ($CDCl_3$): δ 8.11-8.04 (m, 1H), 7.73-7.68 (m, 1H), 7.57-7.49 (m, 2H), 3.38 (s, 3H), 3.19-3.15 (br s, 4H), 1.55-1.50 (br s, 6H); ^{13}C NMR ($CDCl_3$): δ 153.4, 150.5, 145.6, 134.6, 130.5, 129.4, 128.9, 125.8, 125.7, 48.8 (2C), 38.4, 25.3 (2C), 24.1; ESI-MS: 364.05 $[M + H]^+$

4-(Piperidin-1-yl)-1,2,5-thiadiazol-3-yl (4-cyanophenyl)(methyl)carbamate (40)

White solid (333 mg, 60%); ^{1}H NMR ($CDCl_3$): δ 7.71 (d, J = 8.65 Hz, 2H), 7.50 (d, J = 8.95 Hz, 2H), 3.48 (s, 3H), 3.29-3.24 (br s, 4H), 1.62-1.57 (br s, 6H); ^{13}C NMR ($CDCl_3$): δ 153.5, 150.5, 145.9, 145.6, 133.2, 126.2, 118, 110.8, 49 (2C), 38, 25.3, 25.1, 24; ESI-MS: 344.05 $[M + H]^+$

4-(Piperidin-1-yl)-1,2,5-thiadiazol-3-yl (4-chlorophenyl)(methyl)carbamate (41)

White solid (290 mg, 51%); ^{1}H NMR ($CDCl_3$): δ 7.38-7.26 (m, 4H), 3.41-3.37 (m, 4H), 3.20 (s, 3H), 1.60-1.57 (m, 6H); ^{13}C NMR ($CDCl_3$): δ 153.5, 150.8, 146, 140.5, 133.4, 129.5 (2C), 127.8, 126.3, 49.7, 48.9, 38.6, 25.5 (2C), 24.1; ESI-MS: 353.03 $[M + H]^+$

4-(Piperidin-1-yl)-1,2,5-thiadiazol-3-yl (4-fluorophenyl)(methyl)carbamate (42)

White solid (250 mg, 46%); ^{1}H NMR ($CDCl_3$): δ 7.30-7.01 (m, 4H), 3.42-3.36 (m, 4H), 3.24-3.17 (m, 3H), 1.63-1.55 (m, 6H);^{13}C NMR ($CDCl_3$): δ 162.6, 160.6, 153.4, 151, 146.1, 138, 128.3, 127, 116.4, 48.9, 38.9, 29.7, 25.4, 25.3, 24.1; ESI-MS: 337.12 $[M + H]^+$

4-(Piperidin-1-yl)-1,2,5-thiadiazol-3-yl (3-fluorophenyl)(methyl)carbamate (43)

White solid (500 mg, 50%); ^{1}H NMR ($CDCl_3$): δ 7.39-7.36 (m, 1H), 7.15-7.02 (m, 3H), 3.42 (s, 3H), 3.26-3.22 (m, 4H), 1.59-1.55 (m, 6H);^{13}C NMR ($CDCl_3$): δ 163.7, 161.8, 153.5, 150.8, 147, 143.5, 130.5 (3C), 49 (2C), 29.7, 25.4 (2C), 24.2; ESI-MS: 337.12 $[M + H]^+$

4-(Piperidin-1-yl)-1,2,5-thiadiazol-3-yl methyl (p-tolyl)carbamate (44)

White solid (110 mg, 20%); ^{1}H NMR ($CDCl_3$): δ 7.28-7.19 (m, 4H), 3.39-3.35 (m, 4H), 3.19 (s, 3H), 2.38 (s, 3H), 1.62-1.55 (m, 6H); ^{13}C NMR ($CDCl_3$): δ 153.5, 151.1, 146.3, 139.4, 137.6, 130, 126.2, 49.2, 48.8 (2C), 38.8, 25.6, 25.4 (2C), 24.1, 21; ESI-MS: 333.06 $[M + H]^+$

4-(Piperidin-1-yl)-1,2,5-thiadiazol-3-yl methyl(m-tolyl)carbamate (45)

Colorless oil (290 mg, 40%); ^{1}H NMR ($CDCl_3$): δ 7.27 (d, J = 7.17 Hz, 1H), 7.15-7.10 (br s, 3H), 3.40-3.35 (br s, 3H), 3.23-3.17 (br s, 4H), 2.39-2.34 (s, 3H), 1.58-1.53 (br s, 6H); ^{13}C NMR ($CDCl_3$): δ 153.6, 151.1, 146.3, 142, 139.5, 129.2, 128.5, 127.2, 123.6, 48.9 (2C), 38.8, 25.5 (2C), 24.2, 21.3; ESI-MS: 333.06 $[M + H]^+$

4-(Piperidin-1-yl)-1,2,5-thiadiazol-3-yl methyl(o-tolyl)carbamate (46)

White solid (233 mg, 32%); ^{1}H NMR ($CDCl_3$): δ 7.28-7.20 (m, 4H), 3.31 (s, 3H), 3.17-3.14 (br s, 4H), 2.35 (s, 3H), 1.55-1.49 (br s, 6H); ^{13}C NMR ($CDCl_3$): δ 153.4, 151.2, 146.2, 140.6, 135.4, 131.2 (2C), 128.4, 127.1, 49.1, 48.8, 37.7, 25.4 (2C), 24.2, 17.5; ESI-MS: 333.08 $[M + H]^+$

4-(Piperidin-1-yl)-1,2,5-thiadiazol-3-yl (4-methoxyphenyl)(methyl)carbamate (47)

White solid (290 mg, 52%); ^{1}H NMR ($CDCl_3$): δ 7.22 (d, J = 8.05 Hz, 2H), 6.90 (d, J = 8.81 Hz, 2H), 3.81 (s, 3H), 3.35 (s, 3H), 3.22-3.17 (br s, 4H), 1.61-1.58 (br s, 6H); ^{13}C NMR ($CDCl_3$): δ 158.7, 153.4, 151.2, 146.2, 134.7, 127.6, 126.3, 114.4 (2C), 55.4, 48.8 (2C), 39, 25.5, 25.3, 24.1; ESI-MS: 349.04 $[M + H]^+$

4-(Piperidin-1-yl)-1,2,5-thiadiazol-3-yl (3-methoxyphenyl)(methyl)carbamate (48)

White solid (600 mg, 80%); ^{1}H NMR ($CDCl_3$): δ 7.34-7.28 (m, 1H), 6.94-6.87 (m, 3H), 3.83 (s, 3H), 3.42 (d, J = 8.9 Hz, 7H), 1.71-1.65 (br s, 6H); ^{13}C NMR ($CDCl_3$): δ 160.2, 153.4, 151, 146.1, 143.1, 130 (2C), 118.6, 113, 112.5, 55.4, 48.8, 38.6, 29.6, 25.1, 24.1; ESI-MS: 349.07 $[M + H]^+$

4-(Piperidin-1-yl)-1,2,5-thiadiazol-3-yl (2-methoxyphenyl)(methyl)carbamate (49)

White solid (102 mg, 15%); ^{1}H NMR ($CDCl_3$): δ 7.35-7.27 (m, 2H), 6.99-6.97 (m, 2H), 3.88 (s, 3H), 3.31 (s, 3H), 3.26-3.21 (br s, 4H), 1.58-1.52 (br s, 6H); ^{13}C NMR ($CDCl_3$): δ 154.9, 153.2, 151.5, 146.2, 130.5, 129.4, 128.6, 120.8, 112.1, 55.6, 49, 48.6, 37.7, 25.1 (2C), 24.1; ESI-MS: 349.01 $[M + H]^+$

4-(Piperidin-1-yl)-1,2,5-thiadiazol-3-yl [1,1′-biphenyl]-3-yl(methyl)carbamate (50)

White solid (280 g, 60%); ^{1}H NMR ($CDCl_3$): δ 7.57-7.52 (m, 4H), 7.48-7.43 (m, 3H), 7.37 (t, J = 7.25 Hz, 1H), 7.32-7.28 (m, 1H), 3.45 (s, 3H), 3.22-3.17 (br s, 4H), 1.51-1.48 (br s, 6H); ^{13}C NMR ($CDCl_3$): δ 153.5, 151, 146.2, 142.8, 142.6, 140, 129.7, 129 (3C), 127.9, 127.1 (2C), 126.4, 125.2, 53.4 (2C), 38, 25.3, 25.1, 24; ESI-MS: 395.03 $[M + H]^+$

4-(Piperidin-1-yl)-1,2,5-thiadiazol-3-yl mesityl(methyl)carbamate (51)

White solid (233 mg, 30%); ^{1}H NMR ($CDCl_3$): δ 6.91 (s, 2H), 3.24 (s, 3H), 3.19-3.14 (br s, 4H), 2.29 (d, J = 5.15 Hz, 9H), 1.58-1.53 (br s, 6H); ^{13}C NMR ($CDCl_3$): δ 153.5, 151.6, 146.4, 137.9, 136.9, 136, 135 (2C), 129.4, 129.3, 49.1, 48.7, 36.3, 25.4 (2C), 24.1, 20.9, 17.5 (2C); ESI-MS: 361.06 $[M + H]^+$

4-(Piperidin-1-yl)-1,2,5-thiadiazol-3-yl cyclohexyl(methyl)carbamate (52)

White solid (118 mg, 19%); ^{1}H NMR ($CDCl_3$): δ 4.02-3.97 (m, 1H), 3.42-3.37 (br s, 4H), 2.95-2.91 (d, 3H, two conformations), 1.87-1.77 (m, 4H), 1.75-1.58 (m, 8H), 1.53-1.33 (m, 4H); ^{13}C NMR ($CDCl_3$): δ 153.9, 151.8, 146.8, 56.3, 49 (2C), 30.7, 29.9, 29.7, 25.7, 25.5, 25.4 (2C), 25.3, 24.2; ESI-MS: 325.06 $[M + H]^+$

4-(Piperidin-1-yl)-1,2,5-thiadiazol-3-yl cycloheptyl(methyl)carbamate (53)

White solid (175 mg, 22%); ^{1}H NMR ($CDCl_3$): δ 4.16-4.14 (m, 1H), 3.43-3.39 (br s, 4H), 2.96-2.90 (d, 3H, two conformations), 1.91-1.86 (br s, 2H), 1.74-1.66 (m, 12H), 1.57-1.51 (m, 4H); ^{13}C NMR ($CDCl_3$): δ 153.9, 151.5, 146.8, 58.3, 49 (2C), 32.9, 32.3, 31, 29.7, 29.4, 27.5, 25.4, 25.2, 25.1, 24.2; ESI-MS: 339.08 $[M + H]^+$

4-(Piperidin-1-yl)-1,2,5-thiadiazol-3-yl cyclooctyl(methyl)carbamate (54)

White solid (42 mg, 11%); ^{1}H NMR ($CDCl_3$): δ 4.30-4.26 (m, 1H), 3.44-3.39 (br s, 4H), 2.95-2.89 (d, 3H, two conformations), 1.90-1.72 (m, 6H), 1.69-1.51 (m, 14H); ^{13}C NMR ($CDCl_3$): δ 153.9, 151.6, 146.8, 56.9, 49 (2C), 32.1, 31.4, 29.7, 26.3, 26.1, 25.5, 25.4 (2C), 24.9 (2C), 24.2; ESI-MS: 353.09 $[M + H]^+$

4-Morpholino-1,2,5-thiadiazol-3-yl cyclooctyl(methyl)carbamate (55)

White solid (71 mg, 17%); ^{1}H NMR ($CDCl_3$): δ 4.27-4.22 (m, 1H), 3.81-3.79 (m, 4H), 3.45-3.44 (m, 4H), 2.94-2.89 (d, 3H, two conformations), 1.78-1.70 (m, 6H), 1.67-1.51 (m, 8H); ^{13}C NMR ($CDCl_3$): δ 153.2, 151.5, 146.8, 66.4 (2C), 57.1, 48.2, 48.1, 32.2, 31.4, 29.8, 26.3 (2C), 26, 25, 24.9; ESI-MS: 355.02 $[M + H]^+$

In vitro assays

Determination of ABHD6 activity and reversibility using a sensitive fluorescent glycerol assay—Glycerol liberated from 1-AG hydrolysis was determined with a sensitive fluorescent glycerol assay using lysates of HEK293 cells expressing hABHD6 as previously described.[14,28] In this approach, glycerol production was coupled via a three-step enzymatic cascade to hydrogen peroxide (H_2O_2) dependent generation of resorufin whose fluorescence (λ_{ex} 530; λ_{em} 590 nm) was kinetically monitored using a Tecan Infinite M200 plate reader (Tecan Group Ltd., Männedorf, Switzerland). Briefly, hABHD6-HEK lysates (99 μL, 0.3 μg protein/well) were pretreated for 30 min with the solvent (DMSO) or the inhibitor (1 μL, four to five different concentrations spanning the range 10^{-9} M to 10^{-5} M), after which 1-AG (100 μL, 12.5 μM final concentration) was added and the reaction kinetically monitored for 90 min. The assays routinely contained 0.5% (w/v) BSA (essentially fatty acid free) as a carrier. 1-AG was used instead of 2-AG, as this is the preferred endocannabinoid isomer for hABHD6. [14] The IC_{50}-values at time-point 90 min were calculated after nonlinear fitting of the inhibitor dose-response curves. Assay blanks without enzyme were included in each experiment and fluorescence of the assay blank was subtracted before calculation of the final results. Reversibility of compounds to inhibit hABHD6 were tested in 96-well plate format using a 40-fold-dilution method previously described for testing reversibility of MAGL inhibitors. [28]

Determination of FAAH activity using anandamide as a substrate—Inhibitory activities of the synthesized compounds were determined using membranes of COS-7 cells expressing hFAAH, essentially as previously described.[33] The assay buffer was 50 mM Tris-HCl (pH 7.4); 1 mM EDTA and the test compounds were dissolved in DMSO (the final DMSO concentration was max 5% v/v). The incubations were performed in the presence of 0.5% (w/v) BSA (essentially fatty acid free). Solvent (DMSO) or the inhibitor (5 μL, five to six different concentrations spanning the range 10^{-9} M to 10^{-4} M) was preincubated with protein (55 μL, 1 μg protein/well) for 10 min at 37 °C (60 μL). At the 10 min time point, 20 μM AEA was added so that its final concentration was 2 μM (containing 10 nM of ^{3}H-AEA having specific activity of 60 Ci/mmol and concentration of 1 mCi/mL), and the final incubation volume was 100 μL. The incubations proceeded for 10 min at 37 °C. Ethyl acetate (400 μL) was added at the 20 min time point to stop the enzymatic reaction. Additionally, 100 μl of 50 mM Tris-HCl, pH 7.4; 1 mM EDTA was added. Samples were centrifuged for 4 min at RT 13000 rpm, and aliquots (100 μL) from the aqueous phase containing [ethanolamine 1-^{3}H] were measured for radioactivity by liquid scintillation counting (Wallac 1450 MicroBeta; Wallac Oy, Finland).

Determination of LAL activity using 4-methylumbelliferone oleate as a substrate—LAL activity was determined using a previously described method.[19] Briefly, purified human LAL overexpressed in *Pichia pastoris* (phLAL, 0.01 U/mL, 105 U/mg) was mixed with compounds at 10 μM and preincubated for 20 minutes at 37°C. The reaction was started by addition of 4-methylumbelliferone oleate, which was cleaved by enzymatic activity to 4-methylumbelliferone. The reaction was allowed to proceed for 1h at 37°C, and enzymatic activity was quantified by subtracting background fluorescence from all the values, and results were normalized to the DMSO control value.

Activity-based protein profiling (ABPP) of serine hydrolases—Competitive ABPP using mouse whole brain membranes was conducted to visualize the selectivity of inhibitors towards ABHD6 against other serine hydrolases in brain membrane proteome. We used the active site serine-targeting fluorescent fluorophosphonate probe TAMRA-FP as previously described.[14,28] Briefly, brain membranes (100 μg) were treated for 1 h with DMSO or the selected inhibitors, after which TAMRA-FP labeling was conducted for 1 hour at RT (final probe concentration 2 μM). The reaction was quenched by addition of 2xgel loading buffer, after which 10 μg protein was loaded per lane and the proteins were resolved in 10% SDS-PAGE together with molecular weight standards. TAMRA-FP labeling was visualized (λ_{ex} 552; λ_{em} 575 nm) using a fluorescent scanner (FLA-3000 laser fluorescence scanner, Fujifilm, Tokyo, Japan).

Ethics Statement

For the ABPP experiments in vitro with native mouse brain membrane proteome, membranes prepared from brain tissue of 4-week-old male mice were used. The animals were obtained from the National Laboratory Animal Centre, University of Eastern Finland. The animals were sacrificed using decapitation. Approval for the harvesting of animal tissue was applied, registered and obtained from the local welfare officer of the University of Eastern Finland.

Data analyses

The inhibitor dose-response curves and IC_{50} values derived thereof were calculated from nonlinear regressions using Graph-Pad Prism 5.0 for Windows (GraphPad Software, San Diego California USA, www.graphpad.com) and Matlab.

Molecular Modelling—Molecular modelling was performed using Schrödinger Maestro software package [34] and comparative modelling was done using Accelrys Discovery Studio Client. Structures of small molecules were prepared using the LigPrep module of Schrodinger suite. X-ray crystal structure for the FAAH (pdb:3QK5) [35] and homology model for ABHD6 were used for docking studies. The homology model of ABHD6 is based on 2XMZ template and the model is based on sequence alignment derived from the default blast search (2XMZ [32]: identity 25%, alignment length 269, E-value 1.59373e-12, positive 44%, resolution 1.94 Å). The model was constructed using standard settings of Discovery Studio homology modelling protocol. Side chains of the active site residues were further refined using Prime module of Schrodinger. X-ray structure of the FAAH was pre-processed using the protein preparation wizard of Schrödinger suite in order to optimize the hydrogen bonding network and to remove any possible crystallographic artefacts.[36] Prior to Glide docking studies the grid box was centered using corresponding X-ray ligand as template in the case of FAAH and closest active site residues in the case of ABHD6 model. The Ligand docking was performed using default SP settings of Schrodinger Glide using hydrogen bond constraints to oxyanion hole residues (at least one contact required). Graphical illustrations were generated using MOE software (Molecular Operating Environment (MOE), 2013.8).[37]

Supplementary Material

Refer to Web version on PubMed Central for supplementary material.

Acknowledgments

We thank Ms. Minna Glad, Ms. Tiina Koivunen, Ms. Helly Rissanen, Ms. Taija Hukkanen and Ms. Satu Marttila for their skillful technical assistance. We are grateful to thank Dr. Hong Du (Indiana University School of Medicine) and Dr. Gregory Grabowski (Synageva BioPharma) for the gift of the LAL enzyme. CSC–Scientific Computing, Ltd. is greatly acknowledged for software licenses and computational resources. Graduate School of Drug Design, UEF (for JZP), The Academy of Finland (grants 139140 for TJN, 127653 for TP, 139620 for JTL), Biocenter Finland/DDCB and the National Institutes of Health (grant R37-DK27083) have provided financial support for this study. Part of the research was performed under Marie Curie IEF fellowship for AAK. Part of calculations was performed under computational grant by Interdisciplinary Center for Mathematical and Computational Modeling (ICM), Warsaw, Poland, grant number G30-18. For collaborative purpose we are happy to provide our compound JZP-430 (**55**).

References

1. Blankman JL, Simon GM, Cravatt BF. Chem Biol. 2007; 14:1347–1356. [PubMed: 18096503]
2. Savinainen JR, Saario SM, Laitinen JT. Acta Physiol. 2012; 204:267–276.
3. Tchantchou F, Zhang Y. J Neurotrauma. 2013; 30:565–79. [PubMed: 23151067]
4. Alhouayek M, Masquelier J, Cani PD, Lambert DM, Muccioli GG. Proc Natl Acad Sci U S A. 2013; 110:17558–17563. [PubMed: 24101490]
5. Thomas G, Betters JL, Lord CC, Brown AL, Marshall S, Ferguson D, Sawyer J, Davis MA, Melchior JT, Blume LC, Howlett AC, Ivanova PT, Milne SB, Myers DS, Mrak I, Leber V, Heier C,

Taschler U, Blankman JL, Cravatt BF, Lee RG, Crooke RM, Graham MJ, Zimmermann R, Brown HA, Brown JM. Cell Rep. 2013; 5:508–520. [PubMed: 24095738]

6. Naydenov A, Horne E, Cheah C, Swinney K, Hsu K, Cao J, Marrs W, Blankman J, Tu S, Cherry A, Fung S, Wen A, Li W, Saporito M, Selley D, Cravatt B, Oakley J, Stella N. Neuron. 2014; 83:361–371. [PubMed: 25033180]
7. Lichtman AH, Blankman JL, Cravatt BF. Mol Pharmacol. 2010; 78:993–995. [PubMed: 20952498]
8. Chanda PK, Gao Y, Mark L, Btesh J, Strassle BW, Lu P, Piesla MJ, Zhang M, Bingham B, Uveges A, Kowal D, Garbe D, Kouranova EV, Ring RH, Bates B, Pangalos MN, Kennedy JD, Whiteside GT, Samad TA. Mol Pharmacol. 2010; 78:996–1003. [PubMed: 20855465]
9. Schlosburg JE, Blankman JL, Long JZ, Nomura DK, Pan B, Kinsey SG, Nguyen PT, Ramesh D, Booker L, Burston JJ, Thomas EA, Selley DE, Sim-Selley L, Liu Q, Lichtman AH, Cravatt BF. Nat Neurosci. 2010; 13:1113–1119. [PubMed: 20729846]
10. Fiskerstrand T, H'mida-Ben Brahim D, Johansson S, M'zahem A, Haukanes BI, Drouot N, Zimmermann J, Cole AJ, Vedeler C, Bredrup C, Assoum M, Tazir M, Klockgether T, Hamri A, Steen VM, Boman H, Bindoff LA, Koenig M, Knappskog PM. Am J Hum Genet. 2010; 87:410–417. [PubMed: 20797687]
11. Marrs WR, Blankman JL, Horne EA, Thomazeau A, Lin YH, Coy J, Bodor AL, Muccioli GG, Hu SS, Woodruff G, Fung S, Lafourcade M, Alexander JP, Long JZ, Li W, Xu C, Moeller T, Mackie K, Manzoni OJ, Cravatt BF, Stella N. Nat Neurosci. 2010; 13:951–957. [PubMed: 20657592]
12. Li W, Blankman JL, Cravatt BF. J Am Chem Soc. 2007; 129:9594–9595. [PubMed: 17629278]
13. Marrs WR, Horne EA, Ortega-Gutierrez S, Cisneros JA, Xu C, Lin YH, Muccioli GG, Lopez-Rodriguez M, Stella N. J Biol Chem. 2011; 286:28723–28728. [PubMed: 21665953]
14. Navia-Paldanius D, Savinainen JR, Laitinen JT. J Lipid Res. 2012; 53:2413–2424. [PubMed: 22969151]
15. Bachovchin DA, Ji T, Li W, Simon GM, Blankman JL, Adibekian A, Hoover H, Niessen S, Cravatt BF. Proc Natl Acad Sci U S A. 2010; 107:20941–20946. S20941/1–S20941/172. [PubMed: 21084632]
16. Hsu K, Tsuboi K, Adibekian A, Pugh H, Masuda K, Cravatt BF. Nat Chem Biol. 2012; 8:999–1007. [PubMed: 23103940]
17. Hsu K, Tsuboi K, Chang JW, Whitby LR, Speers AE, Pugh H, Cravatt BF. J Med Chem. 2013; 56:8270–8279. [PubMed: 24152295]
18. Janssen FJ, Deng H, Baggelaar MP, Allarà M, van dW, den Dulk H, Ligresti A, van Esbroeck, Annelot CM, Mc Guire R, Di Marzo V, Overkleeft HS, van dS. J Med Chem. 2014; 57:6610–6622. [PubMed: 24988361]
19. Rosenbaum AI, Cosner CC, Mariani CJ, Maxfield FR, Wiest O, Helquist P. J Med Chem. 2010; 53:5281–5289. [PubMed: 20557099]
20. Mor M, Rivara S, Lodola A, Plazzi PV, Tarzia G, Duranti A, Tontini A, Piersanti G, Kathuria S, Piomelli D. J Med Chem. 2004; 47:4998–5008. [PubMed: 15456244]
21. Long JZ, Jin X, Adibekian A, Li W, Cravatt BF. J Med Chem. 2010; 53:1830–1842. [PubMed: 20099888]
22. Chang J, Niphakis M, Lum K, Cognetta A III, Wang C, Matthews M, Niessen S, Buczynski M, Parsons L, Cravatt B. Chem Biol. 2012; 19:579–588. [PubMed: 22542104]
23. Niphakis MJ, Cognetta AB, Chang JW, Buczynski MW, Parsons LH, Byrne F, Burston JJ, Chapman V, Cravatt BF. ACS Chem Neurosci. 2013; 4:1322–1332. [PubMed: 23731016]
24. Minkkilä A, Saario SM, Nevalainen T. Curr Top Med Chem. 2010; 10:828–858. [PubMed: 20370710]
25. Feledziak M, Lambert DM, Marchand-Brynaert J, Muccioli GG. Recent Pat CNS Drug Discovery. 2012; 7:49–70.
26. Kapanda CN, Poupaert JH, Lambert DM. Curr Med Chem. 2013; 20:1824–1846. [PubMed: 23410152]
27. Blankman JL, Cravatt BF. Pharmacol Rev. 2013; 65:849–871. [PubMed: 23512546]

28. Aaltonen N, Savinainen JR, Ribas CR, Rönkkö J, Kuusisto A, Korhonen J, Navia-Paldanius D, Häyrinen J, Takabe P, Käsnänen H, Pantsar T, Laitinen T, Lehtonen M, Pasonen-Seppänen S, Poso A, Nevalainen T, Laitinen JT. Chem Biol. 2013; 20:379–390. [PubMed: 23521796]
29. Patel JZ, Parkkari T, Laitinen T, Kaczor AA, Saario SM, Savinainen JR, Navia-Paldanius D, Cipriano M, Leppänen J, Koshevoy IO, Poso A, Fowler CJ, Laitinen JT, Nevalainen T. J Med Chem. 2013; 56:8484–8496. [PubMed: 24083878]
30. Savinainen JR, Yoshino M, Minkkilä A, Nevalainen T, Laitinen JT. Anal Biochem. 2010; 399:132–134. [PubMed: 20005861]
31. Bowman AL, Makriyannis A. Chem Biol Drug Des. 2013; 81:382–388. [PubMed: 23110439]
32. Dawson A, Fyfe PK, Gillet F, Hunter WN. BMC Struct Biol. 2011; 11:19. [PubMed: 21513522]
33. Saario SM, Poso A, Juvonen RO, Jaervinen T, Salo-Ahen O. J Med Chem. 2006; 49:4650–4656. [PubMed: 16854070]
34. Schrödinger release 2013-3: Maestro, version 9.6; Ligprep, version 2.8; protein preparation wizard: Epik version 2.6, impact version 6.1, prime version 3.4.; Glide, version 6.1, Schrödinger, LLC, New York, NY, 2013
35. Gustin DJ, Ma Z, Min X, Li Y, Hedberg C, Guimaraes C, Porter AC, Lindstrom M, Lester-Zeiner D, Xu G, Carlson TJ, Xiao S, Meleza C, Connors R, Wang Z, Kayser F. Bioorg Med Chem Lett. 2011; 21:2492–2496. [PubMed: 21392988]
36. Accelrys software inc.. Discovery studio modeling environment, release 4.0. San Diego: Accelrys software inc.; 2013.
37. Molecular operating environment (MOE), 2013.8; chemical computing group Inc., 1010 Sherbooke St. West, Suite #910, Montreal, QC, Canada, H3A 2R7, **2013**.

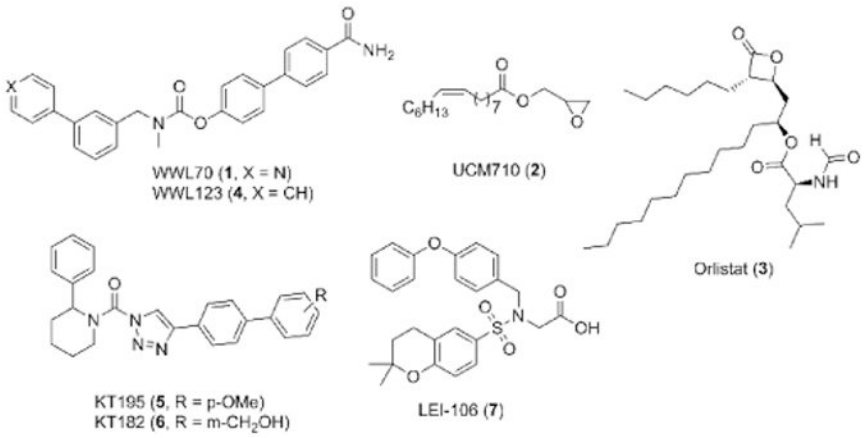

Figure 1. Selective and non-selective ABHD6 inhibitors (1-7)

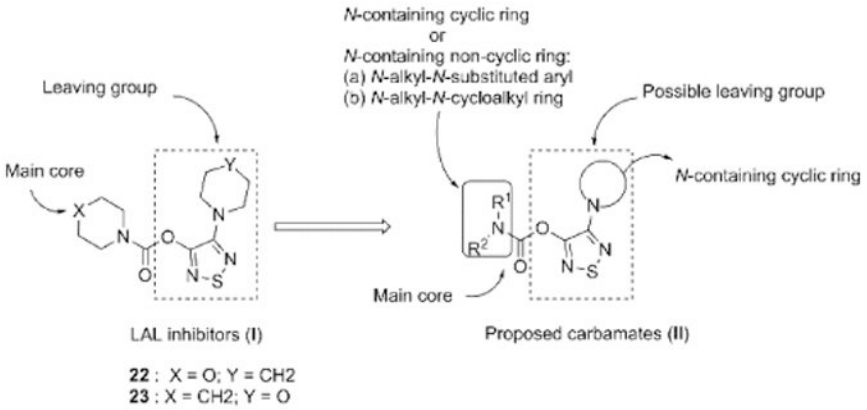

Figure 2. Optimization of 1,2,5-thiadiazole carbamates

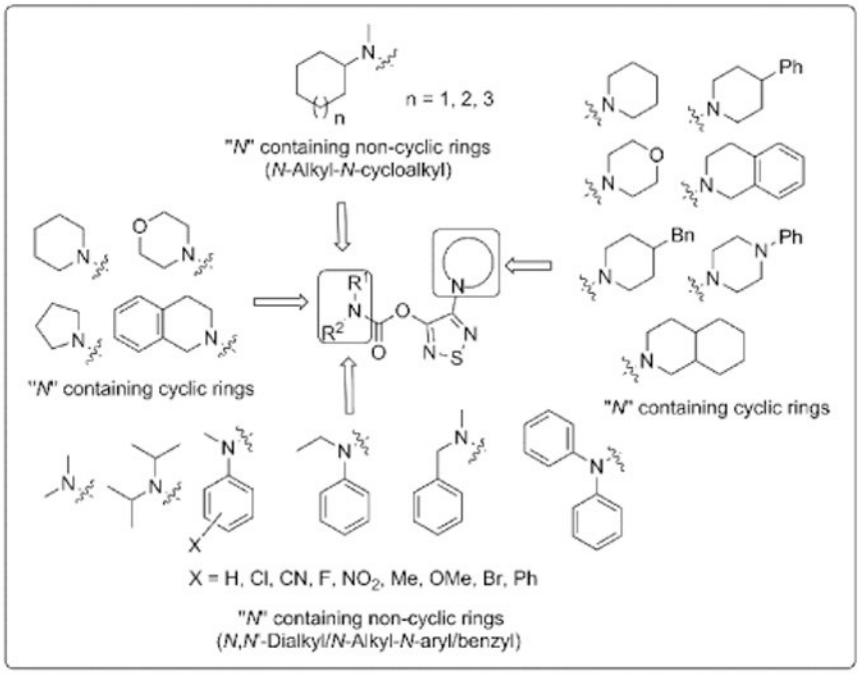

Figure 3. Variations around 1,2,5-thiadiazole scaffold

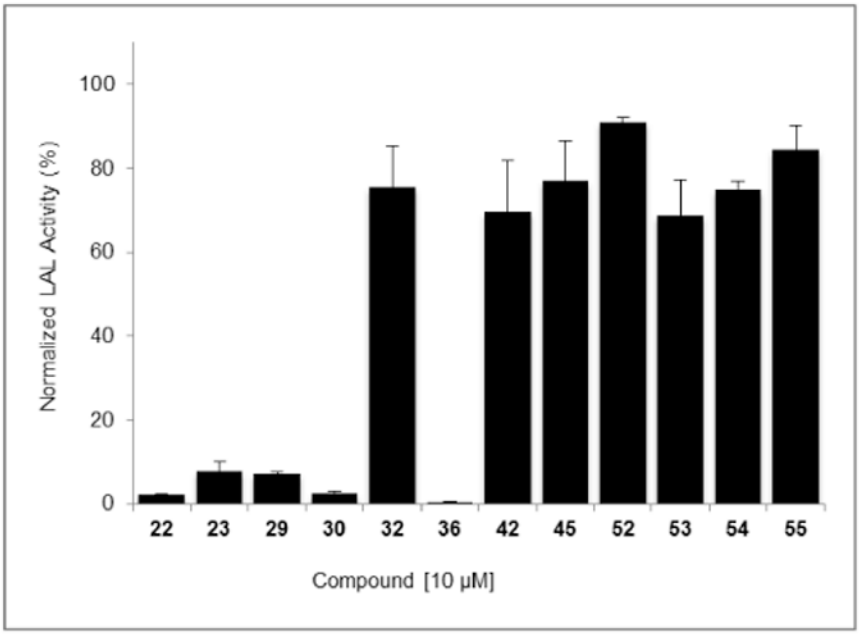

Figure 4.

Lysosomal acid lipase (phLAL) activity in the presence of selected thiadiazole carbamates. Enzymatic activity at 37°C was quantified as background corrected 4-methylumbelliferone fluorescence, normalized to the DMSO control average value. Data are averages ± S.E.M. from two independent experiments (n=5 wells used for quantification per experiment).

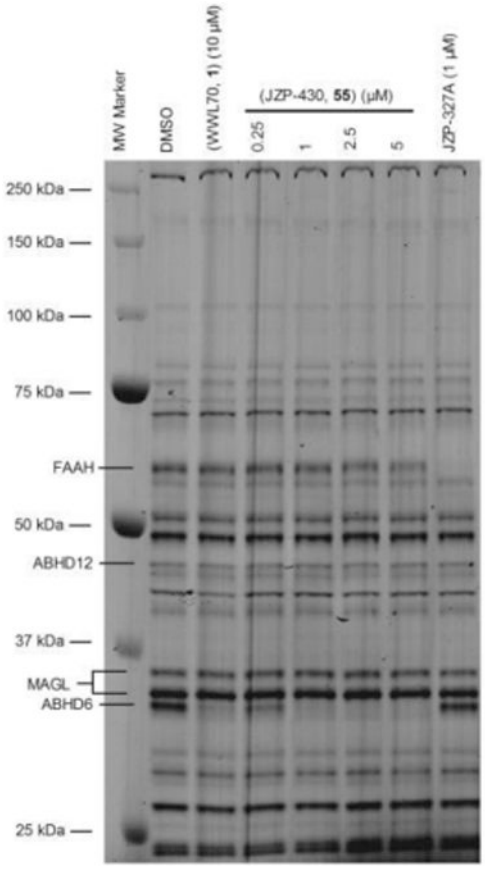

Figure 5.

Competitive ABPP of the compound 55 (JZP-430) among the serine hydrolases in mouse whole brain membrane proteome. Molecular weight markers are indicated at left. Reference inhibitors WWL70 (**1**) and JZP-327A were used at the indicated concentrations to identify the following serine hydrolases from the gel: ABHD6, inhibited by WWL70 (**1**) [12] and FAAH, inhibited by JZP-327A.[29] In addition, protein bands corresponding to MAGL (doublet) and ABHD12 are indicated. Note that JZP-430 (**55**) inhibits only probe labeling of ABHD6 at 0.25 μM concentration. Selective inhibition of ABHD6 was evident at below 2.5 μM concentration while partial inhibition of FAAH was witnessed at 5 μM (20-fold). The gel is representative from two ABPP experiments with similar outcome.

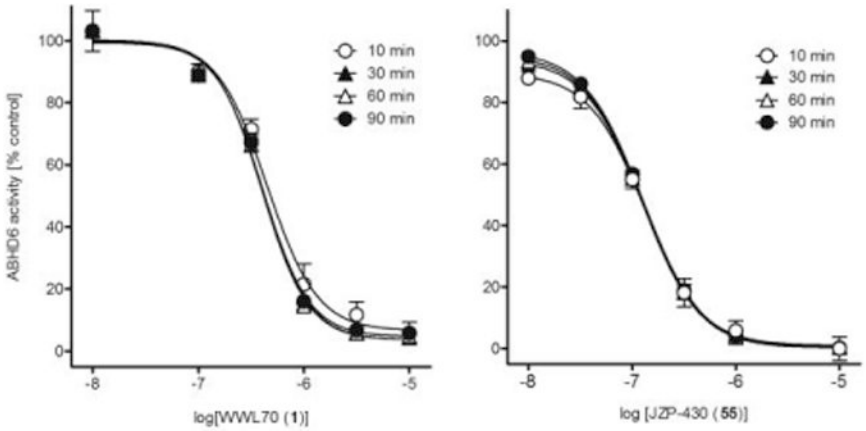

Incubation time	WWL70 (**1**) (pIC_{50} ± SEM)	JZP-430 (**55**) (pIC_{50} ± SEM)
10 min	6.35 ± 0.07	6.88 ± 0.05
30 min	6.39 ± 0.03	6.90 ± 0.02
60 min	6.40 ± 0.03	6.91 ± 0.02
90 min	6.40 ± 0.03	6.90 ± 0.02

Figure 6.

Potencies (pIC_{50}) of the irreversible ABHD6 inhibitor WWL70 (**1**) and compound **55** (JZP-430) are not time-dependently changed following a fast 40-fold dilution of inhibitor-treated hABHD6 preparation indicating that within the time-frame studied, compound **55** acts as an irreversible ABHD6 inhibitor. Note that due to methodological limitations, the IC_{50} values obtained by the dilution method are not directly comparable to those obtained using the routine assay protocol (Table 4). [28,30] Data are mean ± SEM from three independent experiments.

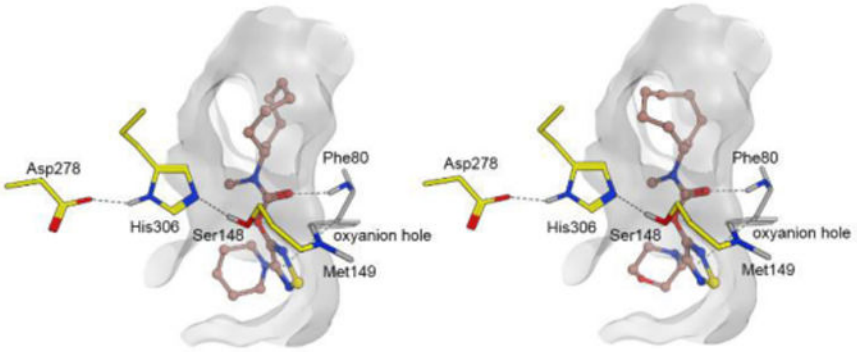

Figure 7.

Most favorable Glide docking poses of high affinity compounds **54** (left) and **55** (JZP-430) (right) to the ABHD6 active site in a homology model. Catalytic residues are colored using yellow carbons and the surface of the active site is presented.

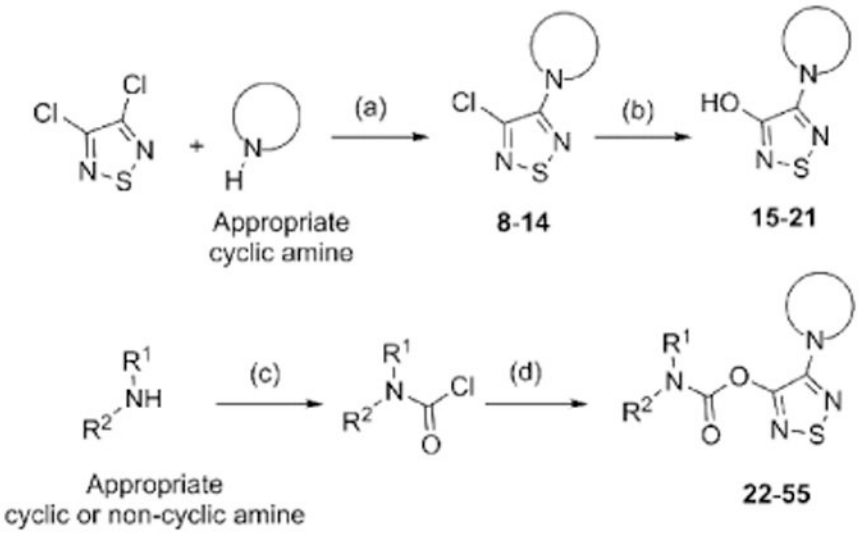

Scheme 1. Synthesis of 1,2,5-thiadiazole carbamate derivatives 22-55[a]

[a] Reagents and conditions: (a) 110-120 °C, 2-6 h or K_2CO_3, DMF, 100-110 °C, 6-10 h; (b) aq. NaOH or KOH, DMSO, reflux, 1-6 h; (c) pyridine, DCM, triphosgene, 0-5 °C or -78 °C, 3-4 h; (d) dry THF, 12-18, KOtBu, 0-25 °C, 16-24 h

Table 1

Inhibitory activities of 1,2,5-thiadiazole carbamates 22–30 against hABHD6 and hFAAH

Compd	Structure	pI_{50} (range) [IC_{50}, μM] [a] or % inhibition at 1 μM [b]	pI_{50} (range) [IC_{50}, μM] [a] or % inhibition at 10 μM [b]
		hABHD6 [μM]	hFAAH [μM]
22	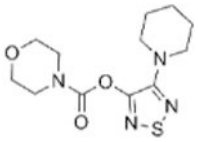	7.28 (7.23-7.32) [0.052]	6.39 (6.29-6.49) [0.40]
23	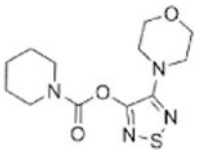	7.07 (7.03-7.10) [0.085]	6.48 (6.41-6.55) [0.30]
24	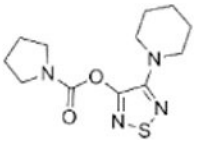	6.58 (6.43-6.73) [0.26]	6.09 (6.01-6.18) [0.81]
25	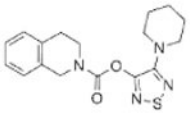	6.88 (6.80-6.95) [0.13]	6.25 (6.23-6.27) [0.56]
26	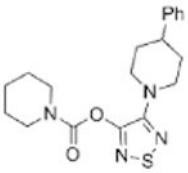	41 %	5.83 (5.34-6.31) [1.47]
27	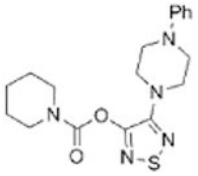	40 %	6.68 (6.51-6.84) [0.21]
28	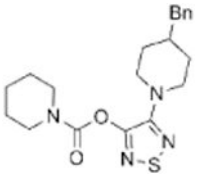	15 %	6.49 (6.30-6.67) [0.32]

Compd	Structure	pI_{50} (range) [IC_{50}, μM] [a] or % inhibition at 1 μM [b]	pI_{50} (range) [IC_{50}, μM] [a] or % inhibition at 10 μM [b]
		hABHD6 [μM]	**hFAAH [μM]**
29	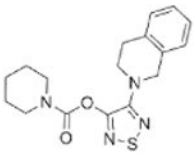	6.34 (6.22-6.45) [0.46]	7.77 (7.71-7.83) [0.017]
30	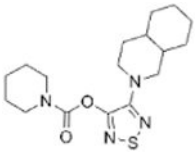	6.25 (6.19-6.31) [0.56]	7.51 (7.48-7.53) [0.031]
WWL70 (**1**)	-----	7.07 ± 0.05 [0.085][c]	30%
THL (**3**)	-----	7.32 ± 0.11 [0.048][c]	NA [d]
JZP-327A[e]	-----	NI[f]	7.94 (7.91–7.97) [0.011]

[a] pI_{50} values ($-\log_{10}$ [IC_{50}]) represent the mean (range) from two independent experiments performed in duplicates. IC_{50} values are calculated for those compounds having ≥50% inhibition at 1 μM for hABHD6, and at 10 μM for hFAAH; and are derived from the mean pI_{50} values as shown in brackets.

[b] The percentage (%) inhibition is represented as the mean from two independent experiments performed in duplicates.

[c] pI_{50} values ($-\log_{10}$ [IC_{50}]) represent the mean ± S.E.M. from three independent experiments performed in duplicates and reported in ref. 13.

[d] NA indicates not analyzed.

[e] JZP-327A, *S*-(-)-3-(1-(4-isobutylphenyl)ethyl)-5-methoxy-1,3,4-oxadiazol-2(3H)-one used as reference FAAH inhibitor reported in ref. 25.

[f] NI indicates no inhibition.

Table 2

Inhibitory activities of novel 1,2,5-thiadiazole carbamates 31–36 against ABHD6 and FAAH

Compd	Structure	pI_{50} ± SEM [IC_{50}, μM][a] or % inhibition at 1 μM[b]	pI_{50} (range) [IC_{50}, μM] [c] or % inhibition at 10 μM [b]
		hABHD6 [μM]	hFAAH [μM]
31	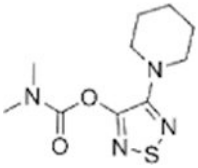	10 %	5.19 (5.17-5.20) [6.45]
32	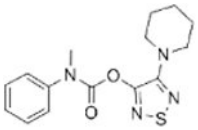	7.66 ± 0.07 [0.022]	5.06 (5.05-5.07) [8.91]
33	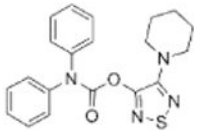	NI [d]	NI
34	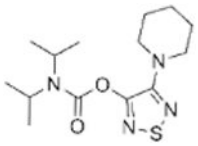	NI	NI
35	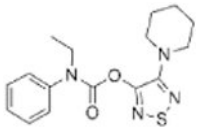	6.33 ± 0.13 [0.47]	24 %
36	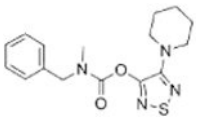	8.01 ± 0.03 [0.010]	7.20 (7.17-7.23) [0.063]

[a] pI_{50} values ($-\log_{10}$ [IC_{50}]) represent the mean ± S.E.M. from three independent experiments performed in duplicates. IC_{50} values are calculated for those compounds having ≥50% inhibition at 1 μM for hABHD6, and at 10 μM for hFAAH; and are derived from the mean pI_{50} values as shown in brackets.

[b] The percentage (%) of inhibition is represented as the mean from two independent experiments performed in duplicates.

[c] pI_{50} values ($-\log_{10}$ [IC_{50}]) represent the mean (range) from two independent experiments performed in duplicates.

[d] NI indicates no inhibition.

Table 3

Inhibitory activities of novel 1,2,5-thiadiazole carbamates 37–51 against ABHD6 and FAAH

Compd	Structure	pI_{50} ± SEM [IC_{50}, μM][a] or % inhibition at 1 μM[b]	% inhibition at 10 μM [b]
		hABHD6 [μM]	hFAAH [μM]
37	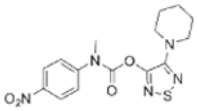	5.90 ± 0.08 [1.25]	19 %
38	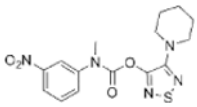	5.92 ± 0.05 [1.20]	11 %
39	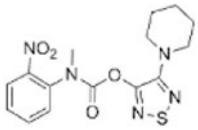	NI[c]	46 %
40	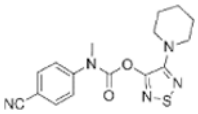	15 %	19 %
41	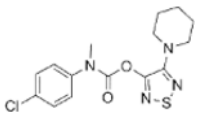	6.39 ± 0.03 [0.41]	16 %
42	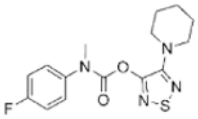	7.11 ± 0.07 [0.078]	22 %
43	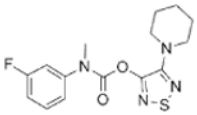	7.22 ± 0.05 [0.060]	48 %
44	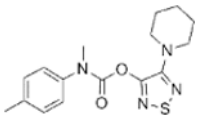	6.83 ± 0.04 [0.15]	21 %
45	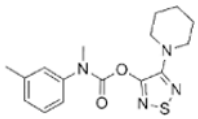	7.27 ± 0.07 [0.054]	9 %

Compd	Structure	pI_{50} ± SEM [IC_{50}, μM][a] or % inhibition at 1 μM[b]	% inhibition at 10 μM [b]
		hABHD6 [μM]	hFAAH [μM]
46	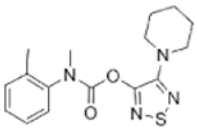	17 %	40 %
47	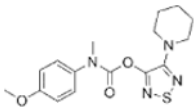	6.58 ± 0.04 [0.26]	17 %
48	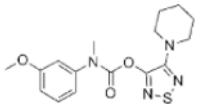	6.71 ± 0.07 [0.19]	17 %
49	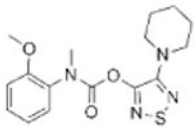	11 %	18 %
50	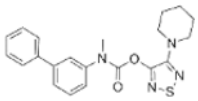	6.04 ± 0.10 [0.91]	13 %
51	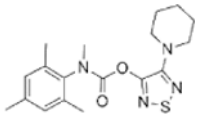	NI	7 %

[a] pI_{50} values ($-\log_{10}$ [IC_{50}]) represent the mean ± S.E.M. from three independent experiments performed in duplicates. IC_{50} values are calculated for those compounds having ≥50% inhibition at 1 μM for hABHD6, and at 10 μM for hFAAH; and are derived from the mean pI_{50} values as shown in brackets.

[b] The percentage (%) of inhibition is represented as the mean from two independent experiments performed in duplicates.

[c] NI indicates no inhibition.

Table 4

Inhibitory activities of novel 1,2,5-thiadiazole carbamates 52–55 against ABHD6 and FAAH

Compd	Structure	pI_{50} ± SEM [IC_{50}, μM][a] or % inhibition at 1 μM[b]	% inhibition at 10 μM [b]
		hABHD6 [μM]	hFAAH [μM]
52	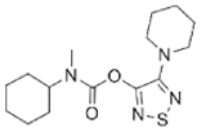	7.36 ± 0.05 [0.044]	16 %
53	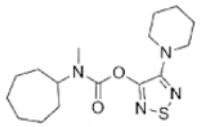	7.37 ± 0.05 [0.043]	21 %
54	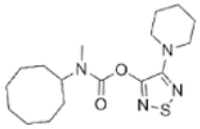	7.14 ± 0.06 [0.072]	13 %
55 (JZP-430)	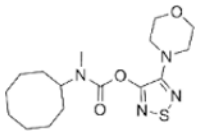	7.36 ± 0.05 [0.044]	18 %

[a] pI_{50} values ($-\log_{10}$ [IC_{50}]) represent the mean ± S.E.M. from three independent experiments performed in duplicates. IC_{50} values are calculated for those compounds having ≥50% inhibition at 1 μM for hABHD6, and at 10 μM for hFAAH; and are derived from the mean pI_{50} values as shown in brackets.

[b] The percentage (%) of inhibition is represented as the mean from two independent experiments performed in duplicates.